

Post-stagnation-point boundary layer flow and mixed convection heat transfer over a vertical, linearly stretching sheet

A. ISHAK¹⁾, R. NAZAR¹⁾, I. POP²⁾

¹⁾ *School of Mathematical Sciences
Faculty of Science and Technology
Universiti Kebangsaan Malaysia
43600 UKM Bangi, Selangor, Malaysia
e-mail: rmn72my@yahoo.com*

²⁾ *Faculty of Mathematics, University of Cluj
R-3400 Cluj, CP 253, Romania*

A THEORETICAL ANALYSIS is made for the steady two-dimensional post-stagnation-point flow of an incompressible viscous fluid over a stretching vertical sheet in its own plane. The stretching velocity, the free stream velocity and the surface temperature are assumed to vary linearly with the distance from the stagnation point. The governing partial differential equations are transformed into a coupled system of ordinary differential equations, which is then solved numerically by a finite-difference method. Results are presented in terms of the skin friction coefficient and local Nusselt number, along with a selection of velocity and temperature profiles. It was shown that for both cases of a fixed surface ($\varepsilon = 0$) and a stretching surface ($\varepsilon \neq 0$), dual solutions exist for the assisting flow (positive values of the buoyancy parameter λ), besides that usually reported in the literature for the opposing flow ($\lambda < 0$). It was also found that for the assisting flow, a solution exists for all values of λ (> 0), while for the opposing flow, a solution exists only if the magnitude of the buoyancy parameter is small.

Notations

a, b, c	constants,
C_f	skin friction coefficient,
f	dimensionless stream function,
g	acceleration due to gravity,
Gr_x	local Grashof number,
k	thermal conductivity,
Nu_x	local Nusselt number,
Pr	Prandtl number,
q_w	local heat flux,
Re_x	local Reynolds number,
T	fluid temperature,
T_w	surface temperature,
T_∞	ambient temperature,

u, v velocity components along the x and y directions, respectively,
 U_∞ free stream velocity along the x -axis far from the stretching sheet,
 U_w velocity of the stretching surface,
 V_∞ free stream velocity along the y -axis far from the stretching sheet,
 x, y Cartesian coordinates along the surface and normal to it, respectively.

Greek Letters

α thermal diffusivity,
 β thermal expansion coefficient,
 ε velocity ratio parameter,
 η similarity variable,
 λ buoyancy or mixed convection parameter,
 θ dimensionless temperature,
 μ dynamic viscosity,
 ν kinematic viscosity,
 ρ fluid density,
 τ_w wall shear stress,
 ψ stream function.

Subscripts

w condition at the stretching sheet,
 ∞ condition far away from the stretching sheet.

Superscript

' differentiation with respect to η .

1. Introduction

THE STRUCTURE OF THE FLOW near a stagnation-point is a fundamental topic in fluid dynamics and it has attracted many investigations during the past several decades because of its wide industrial and technical applications such as cooling of electronic devices by fans, cooling of nuclear reactors during emergency shutdown, heat exchangers placed in a low-velocity environment, solar central receivers exposed to wind currents, and many hydrodynamic processes. HIEMENZ [1] was the first to study the two-dimensional stagnation-point flow and obtained an exact similar solution of the governing Navier–Stokes equations. Since then many investigators have considered various aspects of such flow and obtained similarity solutions. The numerical solution reveals the onset of a wall-vorticity layer, which is a prototype of an “exact” boundary layer distinguished by the absence of the usual boundary layer approximation. In pure forced convection the stagnation point flow results from a two-dimensional flow impinging on a surface at right angle and flowing thereafter symmetrically about the stagnation line. In mixed convection the flow and thermal fields are no longer symmetric with respect to the stagnation line. In addition, the local heat transfer rate and the local shear stress can be significantly enhanced or diminished

in comparison to the pure forced convection flow. The combined forced and free convection (mixed convection) flow is important when the buoyancy forces due to the temperature difference between the surface and the free stream become large, which in turn significantly affected the flow and the thermal fields. RAMACHANDRAN *et al.* [2] studied laminar mixed convection in two-dimensional stagnation flows around heated surfaces by considering both cases of an arbitrary wall temperature and arbitrary surface heat flux variations. They found that a reverse flow develops in the buoyancy opposing flow region, and dual solutions are found to exist for a certain range of the buoyancy parameter. This work was then extended by DEVI *et al.* [3] for unsteady case, and by LOK *et al.* [4] for a vertical surface immersed in a micropolar fluid. Dual solutions were found to exist by these authors for a certain range of the buoyancy parameter. TAKHAR *et al.* [5] studied unsteady mixed convection flow of a viscous incompressible, electrically conducting fluid in the vicinity of a stagnation-point adjacent to a heated vertical surface. Both the constant wall temperature and constant heat flux conditions were considered. However, the existence of dual solutions was not reported in that paper.

All of the above-mentioned investigations considered that the flow impinges normal to a vertical or horizontal surface at rest. The stagnation-point flows towards a surface which is moved or stretched, have been considered for example by CHIAM [6, 7], MAHAPATRA and GUPTA [8, 9] and NAZAR *et al.* [10, 11]. The fluid dynamics due to a stretching surface is important in extrusion processes. The production of sheeting material arises in a number of industrial manufacturing processes and includes both metal and polymer sheets. Examples include the cooling of an infinite metallic plate in a cooling bath, the boundary layer along the material handling conveyers, the aerodynamic extrusion of plastic sheets, the boundary layer along a liquid film in condensation processes, paper production, glass blowing, metal spinning and drawing of plastic films. The quality of the final product depends on the rate of heat transfer at the stretching surface.

In this paper, we present an analysis which may be regarded as an extension of the work of RAMACHANDRAN *et al.* [2], by considering external flow impingement normal towards the stretching vertical surface. The boundary and external flow velocities as well as the surface temperature are assumed to vary linearly with the distance from the stagnation-point. The governing partial differential equations are first transformed into ordinary differential equations using similarity variables and then they are solved numerically by a finite-difference method.

2. Mathematical formulation

Consider a mixed convection boundary layer flow near the stagnation-point on a vertical, heated, linearly stretching sheet in a viscous and incompressible

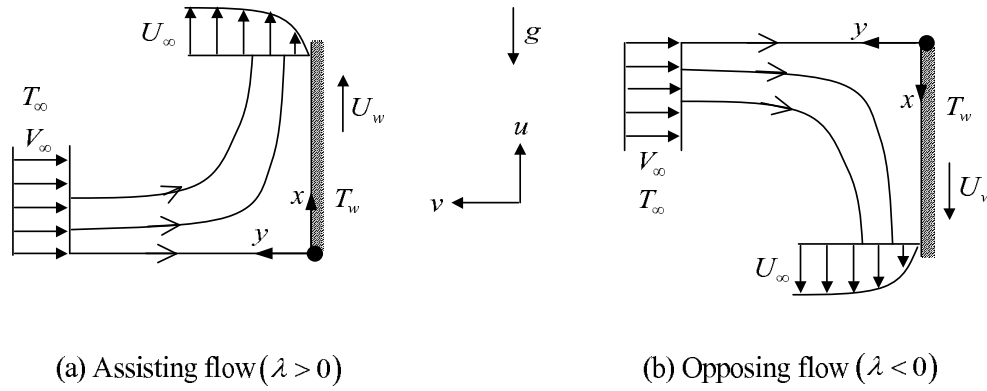


FIG. 1. Physical model and coordinate system.

viscous fluid, as shown in Fig. 1. Cartesian coordinates (x, y) are taken such that the x -axis is measured along the sheet oriented in the upward or downward direction and the y -axis is normal to it. It is assumed that the stretching velocity is given by $U_w(x) = ax$, and the velocity distribution in frictionless potential flow in the neighbourhood of the stagnation point at $x = y = 0$ is given by $U_\infty(x) = bx$, $V_\infty(y) = -by$, while the surface temperature is in the form $T_w(x) = T_\infty + cx$, where a , b and c are positive constants. For Fig. 1(a), the x -axis points upwards in the direction of the stretching surface such that the external flow and the stretching surface induced flow (in the boundary layer) and the thermal buoyant flow assist each other (assisting flow). On the other hand, for Fig. 1(b), the x -axis points vertically downwards in the direction of the stretching surface, but in this case the external flow and the stretching surface induce flow and the thermal buoyant flow oppose each other (opposing flow). Under these assumptions and the Boussinesq approximation, the governing two-dimensional Navier–Stokes and energy equations are (see RAMACHANDRAN *et al.* [2]):

$$(2.1) \quad \frac{\partial u}{\partial x} + \frac{\partial v}{\partial y} = 0,$$

$$(2.2) \quad u \frac{\partial u}{\partial x} + v \frac{\partial u}{\partial y} = -\frac{1}{\rho} \frac{\partial p}{\partial x} + \nu \left(\frac{\partial^2 u}{\partial x^2} + \frac{\partial^2 u}{\partial y^2} \right) \pm g\beta(T - T_\infty),$$

$$(2.3) \quad u \frac{\partial v}{\partial x} + v \frac{\partial v}{\partial y} = -\frac{1}{\rho} \frac{\partial p}{\partial y} + \nu \left(\frac{\partial^2 v}{\partial x^2} + \frac{\partial^2 v}{\partial y^2} \right),$$

$$(2.4) \quad u \frac{\partial T}{\partial x} + v \frac{\partial T}{\partial y} = \alpha \left(\frac{\partial^2 T}{\partial x^2} + \frac{\partial^2 T}{\partial y^2} \right),$$

subject to the boundary conditions

$$(2.5) \quad \begin{aligned} u &= U_w(x), & v &= 0, & T &= T_w(x) & \text{at } y &= 0, \\ u &\rightarrow U_\infty(x), & v &= V_\infty(y), & T &\rightarrow T_\infty & \text{as } y &\rightarrow \infty, \end{aligned}$$

where u and v are the velocity components along the x - and y -axes, respectively, p is the pressure in the flow field, g is the acceleration due to gravity, α is the thermal diffusivity of the fluid, ν is the kinematic viscosity, β is the coefficient of thermal expansion and ρ is the fluid density. The last term on the right-hand side of Eq. (2.2) represents the influence of the thermal buoyancy force on the flow field, with “+” and “-” signs pertaining to the buoyancy assisting and the buoyancy opposing flow regions, respectively.

Further, we eliminate the pressure p from Eqs. (2.2) and (2.3) by cross-differentiation and introduce the stream function ψ defined as $u = \partial\psi/\partial y$ and $v = -\partial\psi/\partial x$, which satisfy the continuity equation (2.1). Thus we get the following equation:

$$(2.6) \quad \frac{\partial\psi}{\partial y} \frac{\partial}{\partial x} (\nabla^2\psi) - \frac{\partial\psi}{\partial x} \frac{\partial}{\partial y} (\nabla^2\psi) = \nu\nabla^4\psi \pm g\beta \frac{\partial T}{\partial y},$$

subject to the boundary conditions

$$(2.7) \quad \begin{aligned} \psi &= 0, & \frac{\partial\psi}{\partial y} &= U_w(x) & \text{at } y &= 0, \\ \frac{\partial\psi}{\partial y} &\rightarrow U_\infty(x), & \frac{\partial\psi}{\partial x} &\rightarrow -V_\infty(y) & \text{as } y &\rightarrow \infty. \end{aligned}$$

Equations (2.4) and (2.6) can be transformed to the corresponding ordinary differential equations by the following transformation (see RAMACHANDRAN *et al.* [2] or CHEN [12]):

$$(2.8) \quad \eta = \left(\frac{U_\infty}{\nu x}\right)^{1/2} y, \quad \psi = (\nu x U_\infty)^{1/2} f(\eta), \quad \theta(\eta) = \frac{T - T_\infty}{T_w - T_\infty}.$$

Substituting (2.8) into Eqs. (2.4) and (2.6), and integrating once the resulting equation from (2.6) with the corresponding boundary conditions, we obtain that the functions $f(\eta)$ and $\theta(\eta)$ are given by the following coupled two ordinary differential equations:

$$(2.9) \quad f''' + f f'' + 1 - f'^2 + \lambda\theta = 0,$$

$$(2.10) \quad \frac{1}{\text{Pr}}\theta'' + f\theta' - f'\theta = 0,$$

where primes denote differentiation with respect to η , $\lambda = \pm \text{Gr}_x / \text{Re}_x^2$ (“±” has the same meaning as in Eq. (2.2)) is the buoyancy or mixed convection

parameter, $\text{Pr} = \nu/\alpha$ is the Prandtl number, $\text{Gr}_x = g\beta(T_w - T_\infty)x^3/\nu^2$ is the local Grashof number and $\text{Re}_x = U_\infty x/\nu$ is the local Reynolds number. Here, $\lambda > 0$ corresponding to the assisting flow, $\lambda < 0$ corresponding to the opposing flow and $\lambda = 0$ corresponds to the forced convection flow. The transformed boundary conditions are:

$$(2.11) \quad \begin{aligned} f(0) &= 0, & f'(0) &= \varepsilon, & \theta(0) &= 1, \\ f'(\eta) &\rightarrow 1, & \theta(\eta) &\rightarrow 0 & \text{as } \eta &\rightarrow \infty, \end{aligned}$$

where $\varepsilon = U_w/U_\infty$ is the velocity ratio parameter.

We note that when $\varepsilon = 0$ (static surface), Eqs. (2.9)–(2.11) reduce to those of RAMACHANDRAN *et al.* [2] for the case of an arbitrary surface temperature with $n = 1$ in their paper.

The physical quantities of interest are the skin friction coefficient C_f and the local Nusselt number Nu_x , which are defined as

$$(2.12) \quad C_f = \frac{\tau_w}{\rho U_\infty^2/2}, \quad \text{Nu}_x = \frac{xq_w}{k(T_w - T_\infty)},$$

where the wall shear stress τ_w and the local heat flux q_w are given by

$$(2.13) \quad \tau_w = \mu \left(\frac{\partial u}{\partial y} \right)_{y=0}, \quad q_w = -k \left(\frac{\partial T}{\partial y} \right)_{y=0},$$

with μ and k being the dynamic viscosity and thermal conductivity, respectively. Using the similarity variables (2.5), we obtain

$$(2.14) \quad \frac{1}{2}C_f \text{Re}_x^{1/2} = f''(0), \quad \text{Nu}_x / \text{Re}_x^{1/2} = -\theta'(0).$$

3. Solution procedure

3.1. Finite-difference method

To solve the transformed differential equations (2.9) and (2.10) subject to the boundary conditions (2.11), Eqs. (2.9) and (2.10) are first converted into a system of five first-order equations, and the difference equations are then expressed using central differences. For this purpose, we introduce new dependent variables $p(\eta)$, $q(\eta)$, $s(\eta) = \theta(\eta)$ and $t(\eta)$ so that Eqs. (2.9) and (2.10) can be written as

$$(3.1) \quad f' = p,$$

$$(3.2) \quad p' = q,$$

$$(3.3) \quad s' = t,$$

$$(3.4) \quad q' + fq + 1 - p^2 + \lambda s = 0,$$

$$(3.5) \quad \frac{1}{\text{Pr}} t' + ft - ps = 0.$$

In terms of the new dependent variables, the boundary conditions (2.11) are given by

$$(3.6) \quad \begin{aligned} f(0) &= 0, & p(0) &= \varepsilon, & s(0) &= 1, \\ p(\eta) &\rightarrow 1, & s(\eta) &\rightarrow 0 & \text{as } \eta &\rightarrow \infty. \end{aligned}$$

We now consider the segment $\eta_{j-1}\eta_j$, with $\eta_{j-1/2}$ as the midpoint, which is defined as below:

$$(3.7) \quad \eta_0 = 0, \quad \eta_j = \eta_{j-1} + h_j, \quad \eta_J = \eta_\infty,$$

where h_j is the $\Delta\eta$ -spacing and $j = 1, 2, \dots, J$ is a sequence number that indicates the coordinate location. The finite-difference approximations to the ordinary differential equations (3.1)–(3.5) are written for the midpoint $\eta_{j-1/2}$ of the segment $\eta_{j-1}\eta_j$. This procedure gives

$$(3.8) \quad \frac{f_j - f_{j-1}}{h_j} = \frac{p_j + p_{j-1}}{2} = p_{j-1/2},$$

$$(3.9) \quad \frac{p_j - p_{j-1}}{h_j} = \frac{q_j + q_{j-1}}{2} = q_{j-1/2},$$

$$(3.10) \quad \frac{s_j - s_{j-1}}{h_j} = \frac{t_j + t_{j-1}}{2} = t_{j-1/2},$$

$$(3.11) \quad \frac{q_j - q_{j-1}}{h_j} + (fq)_{j-1/2} + 1 - (p^2)_{j-1/2} + \lambda s_{j-1/2} = 0,$$

$$(3.12) \quad \frac{1}{\text{Pr}} \frac{t_j - t_{j-1}}{h_j} + (ft)_{j-1/2} - (ps)_{j-1/2} = 0.$$

Rearranging of expressions (3.8)–(3.12) gives

$$(3.13) \quad f_j - f_{j-1} - \frac{1}{2}h_j(p_j + p_{j-1}) = 0,$$

$$(3.14) \quad p_j - p_{j-1} - \frac{1}{2}h_j(q_j + q_{j-1}) = 0,$$

$$(3.15) \quad s_j - s_{j-1} - \frac{1}{2}h_j(t_j + t_{j-1}) = 0,$$

$$(3.16) \quad q_j - q_{j-1} + \frac{1}{4}h_j(f_j + f_{j-1})(q_j + q_{j-1}) + h_j - \frac{1}{4}h_j(p_j + p_{j-1})^2 \\ + \frac{1}{2}\lambda h_j(s_j + s_{j-1}) = 0,$$

$$(3.17) \quad \frac{1}{\text{Pr}}(t_j - t_{j-1}) + \frac{1}{4}h_j(f_j + f_{j-1})(t_j + t_{j-1}) - \frac{1}{4}h_j(p_j + p_{j-1})(s_j + s_{j-1}) = 0.$$

Equations (3.13)–(3.17) are imposed for $j = 1, 2, 3, \dots, J$, and the transformed boundary layer thickness η_J is to be sufficiently large so that it is beyond the edge of the boundary layer. The boundary conditions are

$$(3.18) \quad \begin{aligned} f_0 &= 0, & p_0 &= \varepsilon, & s_0 &= 1, \\ p_J &= 1, & s_J &= 0. \end{aligned}$$

3.2. Newton's method

To linearize the nonlinear system (3.13)–(3.17), we use Newton's method, by introducing the following expressions:

$$(3.19) \quad \begin{aligned} f_j^{(k+1)} &= f_j^{(k)} + \delta f_j^{(k)}, & p_j^{(k+1)} &= p_j^{(k)} + \delta p_j^{(k)}, & q_j^{(k+1)} &= q_j^{(k)} + \delta q_j^{(k)}, \\ s_j^{(k+1)} &= s_j^{(k)} + \delta s_j^{(k)}, & t_j^{(k+1)} &= t_j^{(k)} + \delta t_j^{(k)}, \end{aligned}$$

where $k = 0, 1, 2, \dots$. We then insert the left-hand side expressions in place of f_j, p_j, q_j, s_j and t_j into Eqs. (3.13)–(3.17) and drop the terms that are quadratic in $\delta f^{(k)}, \delta p^{(k)}, \delta q^{(k)}, \delta s^{(k)}$ and $\delta t^{(k)}$. This procedure yields the following linear system (the superscript k is dropped for simplicity):

$$(3.20) \quad \delta f_j - \delta f_{j-1} - \frac{h_j}{2}(\delta p_j + \delta p_{j-1}) = (r_1)_{j-1/2},$$

$$(3.21) \quad \delta p_j - \delta p_{j-1} - \frac{h_j}{2}(\delta q_j + \delta q_{j-1}) = (r_2)_{j-1/2},$$

$$(3.22) \quad \delta s_j - \delta s_{j-1} - \frac{h_j}{2}(\delta t_j + \delta t_{j-1}) = (r_3)_{j-1/2},$$

$$(3.23) \quad \begin{aligned} (a_1)_j \delta q_j + (a_2)_j \delta q_{j-1} + (a_3)_j \delta f_j + (a_4)_j \delta f_{j-1} + (a_5)_j \delta p_j \\ + (a_6)_j \delta p_{j-1} + (a_7)_j \delta s_j + (a_8)_j \delta s_{j-1} = (r_4)_{j-1/2}, \end{aligned}$$

$$(3.24) \quad \begin{aligned} (b_1)_j \delta t_j + (b_2)_j \delta t_{j-1} + (b_3)_j \delta f_j + (b_4)_j \delta f_{j-1} + (b_5)_j \delta p_j + (b_6)_j \delta p_{j-1} \\ + (b_7)_j \delta s_j + (b_8)_j \delta s_{j-1} = (r_5)_{j-1/2}, \end{aligned}$$

where

$$\begin{aligned}
 (3.25) \quad & (a_1)_j = 1 + \frac{1}{2}h_j f_{j-1/2}, & (a_2)_j &= (a_1)_j - 2, \\
 & (a_3)_j = \frac{1}{2}h_j q_{j-1/2}, & (a_4)_j &= (a_3)_j, \\
 & (a_5)_j = -h_j p_{j-1/2}, & (a_6)_j &= (a_5)_j, \\
 & (a_7)_j = \frac{1}{2}\lambda h_j, & (a_8)_j &= (a_7)_j, \\
 & (b_1)_j = \frac{1}{\text{Pr}} + \frac{1}{2}h_j f_{j-1/2}, & (b_2)_j &= (b_1)_j - \frac{2}{\text{Pr}}, \\
 & (b_3)_j = \frac{1}{2}h_j t_{j-1/2}, & (b_4)_j &= (b_3)_j, \\
 & (b_5)_j = -\frac{1}{2}h_j s_{j-1/2}, & (b_6)_j &= (b_5)_j, \\
 & (b_7)_j = -\frac{1}{2}h_j p_{j-1/2}, & (b_8)_j &= (b_7)_j,
 \end{aligned}$$

and

$$\begin{aligned}
 (3.26) \quad & (r_1)_{j-1/2} = -f_j + f_{j-1} + h_j p_{j-1/2}, \\
 & (r_2)_{j-1/2} = -p_j + p_{j-1} + h_j q_{j-1/2}, \\
 & (r_3)_{j-1/2} = -s_j + s_{j-1} + h_j t_{j-1/2}, \\
 & (r_4)_{j-1/2} = -(q_j - q_{j-1}) - h_j (fq)_{j-1/2} - h_j + h_j (p^2)_{j-1/2} - \lambda h_j s_{j-1/2}, \\
 & (r_5)_{j-1/2} = -\frac{1}{\text{Pr}}(t_j - t_{j-1}) - h_j (ft)_{j-1/2} + h_j (ps)_{j-1/2}.
 \end{aligned}$$

The boundary conditions (3.18) become

$$\begin{aligned}
 (3.27) \quad & \delta f_0 = 0, & \delta p_0 &= 0, & \delta s_0 &= 0, \\
 & \delta p_J = 0, & \delta s_J &= 0,
 \end{aligned}$$

which just express the requirement for the boundary conditions to remain constant during the iteration process.

3.3. Block-elimination method

The linearized difference equations (3.20)–(3.24) can be solved by the block-elimination method as outlined by NA [13] and CEBECI and BRADSHAW [14],

$$(3.31) \quad [B_j] = \begin{bmatrix} 0 & 0 & -1 & 0 & 0 \\ 0 & 0 & 0 & -\frac{1}{2}h_j & 0 \\ 0 & 0 & 0 & 0 & -\frac{1}{2}h_j \\ 0 & 0 & (a_4)_j & (a_2)_j & 0 \\ 0 & 0 & (b_4)_j & 0 & (b_2)_j \end{bmatrix}, \quad 2 \leq j \leq J,$$

$$(3.32) \quad [C_j] = \begin{bmatrix} -\frac{1}{2}h_j & 0 & 0 & 0 & 0 \\ 1 & 0 & 0 & 0 & 0 \\ 0 & 1 & 0 & 0 & 0 \\ (a_5)_j & (a_7)_j & 0 & 0 & 0 \\ (b_5)_j & (b_7)_j & 0 & 0 & 0 \end{bmatrix}, \quad 1 \leq j \leq J-1,$$

$$(3.33) \quad [\delta_1] = \begin{bmatrix} \delta q_0 \\ \delta t_0 \\ \delta f_1 \\ \delta q_1 \\ \delta t_1 \end{bmatrix}, \quad [\delta_j] = \begin{bmatrix} \delta p_{j-1} \\ \delta s_{j-1} \\ \delta f_j \\ \delta q_j \\ \delta t_j \end{bmatrix}, \quad 2 \leq j \leq J,$$

and

$$(3.34) \quad [r_j] = \begin{bmatrix} (r_1)_{j-1/2} \\ (r_2)_{j-1/2} \\ (r_3)_{j-1/2} \\ (r_4)_{j-1/2} \\ (r_5)_{j-1/2} \end{bmatrix}, \quad 1 \leq j \leq J.$$

To solve Eq. (3.28), we assume that \mathbf{A} is nonsingular and it can be factorized as

$$(3.35) \quad \mathbf{A} = \mathbf{L}\mathbf{U},$$

where

$$\mathbf{L} = \begin{bmatrix} [\alpha_1] & & & & \\ [B_2] & [\alpha_2] & & & \\ & & \ddots & & \\ & & & \ddots & [\alpha_{J-1}] \\ & & & & [B_J] & [\alpha_J] \end{bmatrix}$$

and

$$\mathbf{U} = \begin{bmatrix} [I] & [T_1] & & & \\ & [I] & [T_2] & & \\ & & & \ddots & \\ & & & & \ddots & \\ & & & & & [I] & [T_{J-1}] \\ & & & & & & [I] \end{bmatrix},$$

where $[I]$ is a 5×5 identity matrix, while $[\alpha_i]$ and $[T_i]$ are 5×5 matrices in which the elements are determined by the following equations:

$$(3.36) \quad [\alpha_1] = [A_1],$$

$$(3.37) \quad [A_1][T_1] = [C_1],$$

$$(3.38) \quad [\alpha_j] = [A_j] - [B_j][T_{j-1}], \quad j = 2, 3, \dots, J,$$

$$(3.39) \quad [\alpha_j][T_j] = [C_j], \quad j = 2, 3, \dots, J-1.$$

Substituting Eq. (3.35) into Eq. (3.28), we obtain

$$(3.40) \quad \mathbf{LU}\boldsymbol{\delta} = \mathbf{r}.$$

If we define

$$(3.41) \quad \mathbf{U}\boldsymbol{\delta} = \mathbf{W},$$

Eq. (3.40) becomes

$$(3.42) \quad \mathbf{LW} = \mathbf{r},$$

where

$$\mathbf{W} = \begin{bmatrix} [W_1] \\ [W_2] \\ \vdots \\ [W_{J-1}] \\ [W_J] \end{bmatrix},$$

and $[W_j]$ are 5×1 column matrices. The elements of \mathbf{W} can be determined from Eq. (3.41) by the following relations:

$$(3.43) \quad [\alpha_1][W_1] = [r_1],$$

$$(3.44) \quad [\alpha_j][W_j] = [r_j] - [B_j][W_{j-1}], \quad 2 \leq j \leq J.$$

When the elements of \mathbf{W} have been found, Eq. (3.41) gives the solution for δ in which the elements are found from the following relations:

$$(3.45) \quad [\delta_J] = [W_J],$$

$$(3.46) \quad [\delta_j] = [W_j] - [I_j][\delta_{j+1}], \quad 1 \leq j \leq J-1.$$

Once the elements of δ are found, Eqs. (3.20)–(3.24) can be used to find the $(k+1)$ th iteration in Eq. (3.19). These calculations are repeated until the convergence criterion is satisfied. In laminar boundary layer calculation, the wall shear stress parameter $q(0)$ is commonly used as the convergence criterion [15]. This is probably because in boundary layer calculations, it is found that the greatest error usually appears in the wall shear stress parameter. Thus, this convergence criterion is used in the present study. Calculations are stopped when

$$(3.47) \quad |\delta q_0^{(k)}| < \epsilon_1,$$

where ϵ_1 is a small prescribed value. In this study, $\epsilon_1 = 0.00001$ is used, which gives about four decimal places accuracy for most of the predicted quantities as suggested in [14, 15].

The present method has a second-order accuracy, unconditionally stable and is easy to be programmed, thus making it highly attractive for production use. The only disadvantage is the large amount of once-and-for-all algebra needed to write the difference equations and to set up their solutions [16].

4. Results and discussion

The step size $\Delta\eta$ in η , and the position of the edge of the boundary layer η_∞ have to be adjusted for different values of the parameters to maintain accuracy. In this study, the values of $\Delta\eta$ between 0.001 and 0.1 were used, depending on the values of the parameters used, in order that the numerical values obtained should be independent of $\Delta\eta$ chosen, at least to four decimal places. However, a uniform grid of $\Delta\eta = 0.01$ was found to be satisfactory for a convergence criterion of 10^{-5} which gives accuracy to four decimal places, in nearly all cases. On the other hand, the boundary layer thickness η_∞ between 4 and 50 was chosen where the infinity boundary condition is achieved. To assess the accuracy of the present method, comparison with the previously reported data available in the open literature is made. The comparisons for the values of the skin friction coefficient $f''(0)$ and the local Nusselt number $-\theta'(0)$ are shown in Tables 1 and 2 respectively, and they are found to be in a very good agreement. The present method is unconditionally stable and has been successfully used by the present authors to solve various problem in fluid mechanics and heat transfer (cf. [17–19]).

Table 1. Values of $f''(0)$ for various values of Pr when $\varepsilon = 0$ (for upper branch solution).

Pr	RAMACHANDRAN <i>et al.</i> [2]		LOK <i>et al.</i> [4]		Present results	
	$\lambda = -1$	$\lambda = 1$	$\lambda = -1$	$\lambda = 1$	$\lambda = -1$	$\lambda = 1$
0.7	0.6917	1.7063	0.691693	1.706376	0.6917	1.7063
7	0.9235	1.5179	0.923528	1.517952	0.9235	1.5179
20	1.0031	1.4485	1.003158	1.448520	1.0031	1.4485
40	1.0459	1.4101	1.045989	1.410094	1.0459	1.4101
60	1.0677	1.3903	1.067703	1.390311	1.0677	1.3903
80	1.0817	1.3774	1.081719	1.377429	1.0817	1.3774
100	1.0918	1.3680	1.091840	1.368070	1.0918	1.3680

Table 2. Values of $-\theta'(0)$ for various values of Pr when $\varepsilon = 0$ (for upper branch solution).

Pr	RAMACHANDRAN <i>et al.</i> [2]		LOK <i>et al.</i> [4]		Present results	
	$\lambda = -1$	$\lambda = 1$	$\lambda = -1$	$\lambda = 1$	$\lambda = -1$	$\lambda = 1$
0.7	0.6332	0.7641	0.633269	0.764087	0.6332	0.7641
7	1.5403	1.7224	1.546374	1.722775	1.5403	1.7224
20	2.2683	2.4576	2.269380	2.458836	2.2683	2.4576
40	2.9054	3.1011	2.907781	3.103703	2.9054	3.1011
60	3.3527	3.5514	3.356338	3.355404	3.3527	3.5514
80	3.7089	3.9095	3.713824	3.914882	3.7089	3.9095
100	4.0097	4.2116	4.015974	4.218462	4.0097	4.2116

To conserve space, we consider the Prandtl number unity throughout the paper, except for comparison with the previously investigated cases. From Tables 1 and 2, it can be seen that for both the assisting and opposing flow cases, as Pr increases, the local Nusselt number increases and it leads to a decrease in the thickness of the thermal region near the fixed surface. The reverse trend is seen for the skin friction coefficient, which decreases as Pr increases when the flow is assisted ($\lambda > 0$). This is due to the increased velocity caused by the assisting buoyancy forces. However, it increases with Pr when the flow is opposing ($\lambda < 0$).

The variations of the skin friction coefficient $f''(0)$ and the local Nusselt number $-\theta'(0)$ with buoyancy parameter λ for $\varepsilon = 0$ and $\varepsilon = 0.1$ are shown in Figs. 2

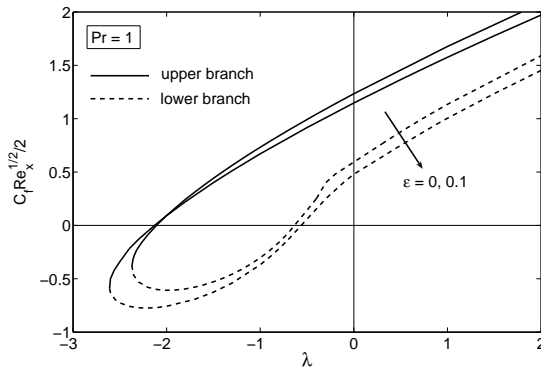


FIG. 2. Skin friction coefficient $\frac{1}{2}C_f Re_x^{1/2} (= f''(0))$ as a function of λ for $\varepsilon = 0$ and $\varepsilon = 0.1$.

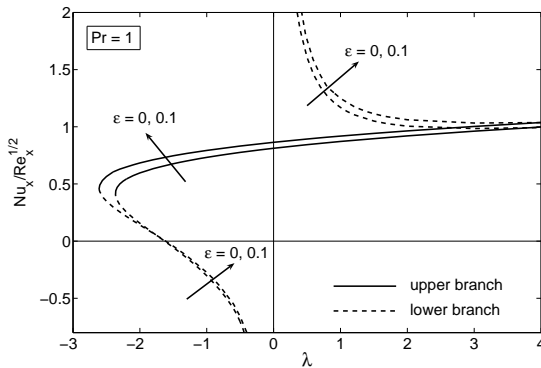


FIG. 3. Local Nusselt number $Nu_x / Re_x^{1/2} (= -\theta'(0))$ as a function of λ for $\varepsilon = 0$ and $\varepsilon = 0.1$.

and 3, respectively. These figures show that it is possible to obtain dual solutions of the similarity equations (2.9)–(2.11) for the assisting flow ($\lambda > 0$), as well as for the opposing flow ($\lambda < 0$) that have been reported by RAMACHANDRAN *et al.* [2], DEVI *et al.* [3] and LOK *et al.* [4]. For $\lambda > 0$, there is a favourable pressure gradient due to the buoyancy forces, which results in the flow being accelerated and consequently there is a larger skin friction coefficient than in the non-buoyant case ($\lambda = 0$). For negative values of λ , there is a critical value λ_c , with two solution branches for $\lambda > \lambda_c$, a saddle-node bifurcation at $\lambda = \lambda_c$ and no solutions for $\lambda < \lambda_c$. Based on our computations, $\lambda_c = -2.364$ for $\varepsilon = 0$ and $\lambda_c = -2.612$ for $\varepsilon = 0.1$. The boundary-layer separates from the surface at $\lambda = \lambda_c$, where $f''(0) < 0$, a different result from the classical boundary-layer theory where separation occurs when $f''(0)$ is zero. This observation is in agreement with the cases reported by RAMACHANDRAN *et al.* [2], DEVI *et al.* [3], LOK *et al.* [4], SCHNEIDER and WASEL [20], and SEARS and TELIONIS [21], who suggested that

the name “separation” should not be given to vanishing wall-shear. Moreover, Figs. 2 and 3 show that the flow separation is delayed if the sheet is stretched. Further, it should be mentioned that the existence of dual solutions in mixed convection boundary layer flow was pointed out by AFZAL and HUSSAIN [22] and HOGG *et al.* [23]. As discussed by AFZAL and HUSSAIN [22], it seems plausible that depending on the manner in which the temperature field is imposed, one or the other dual solutions could be approached after different adjustment phases, causing the solution in the vicinity of the separation region to be dual.

We identify the upper and lower branch solutions in the following discussion by how they appear in Fig. 2, i.e. the upper branch solution has higher values of $f''(0)$ for a given λ than the lower branch solution. As shown in Fig. 3, for the upper branch solutions, the heat transfer rate increases with λ since the skin friction increases, whereas for the lower branch solutions, it becomes discontinuous and unbounded at $\lambda = 0$. It is not possible to determine which solution would occur in practice since a stability analysis has not been done. However, we expect the upper branch solution to be stable and physically relevant, whereas the lower branch is unstable and not physically relevant, since it is the only solution for the case $\lambda = 0$ (cf. Fig. 3). The saddle-node bifurcation at $\lambda = \lambda_c$ corresponds to a change in the (temporal) stability of the solution and, unless there is a change in stability on the upper branch for $\lambda \neq \lambda_c$, the saddle-node bifurcation gives a change in stability from stable (upper branch) to unstable (lower branch). Although the lower branch solutions seem to deprive of physical significance, they are nevertheless of interest so far as the differential equations are concerned. Similar results may arise in other situations where the corresponding solutions have more realistic meaning (see RIDHA [24]).

Figures 4 and 5 respectively present some samples of velocity and temperature profiles for $\lambda = -1$ (opposing flow), while the corresponding profiles for

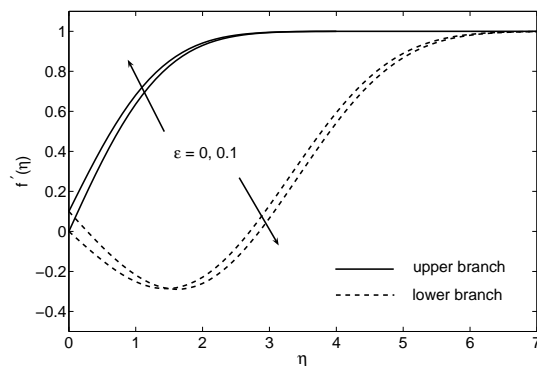


FIG. 4. Velocity profiles $f'(\eta)$ for $\varepsilon = 0$ and $\varepsilon = 0.1$ when $\lambda = -1$ (opposing flow).

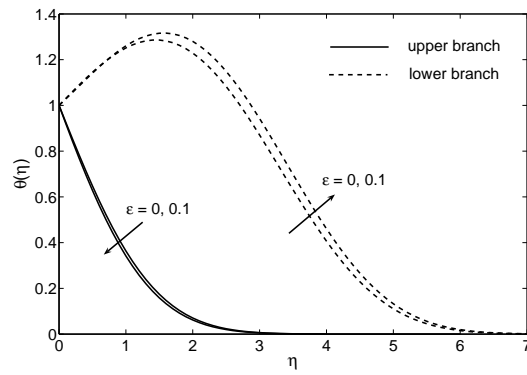


FIG. 5. Temperature profiles $\theta(\eta)$ for $\varepsilon = 0$ and $\varepsilon = 0.1$ when $\lambda = -1$ (opposing flow).

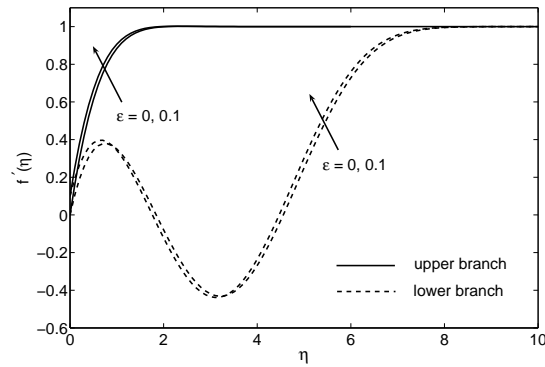


FIG. 6. Velocity profiles $f'(\eta)$ for $\varepsilon = 0$ and $\varepsilon = 0.1$ when $\lambda = 1$ (assisting flow).

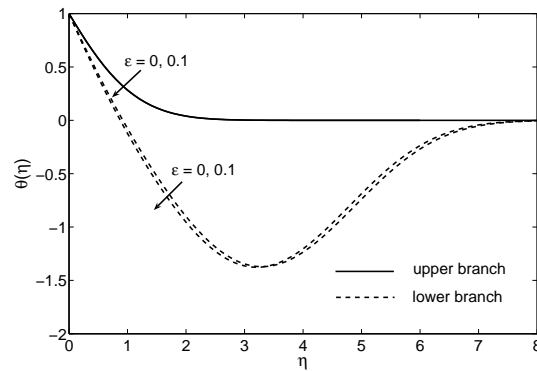


FIG. 7. Temperature profiles $\theta(\eta)$ for $\varepsilon = 0$ and $\varepsilon = 0.1$ when $\lambda = 1$ (assisting flow).

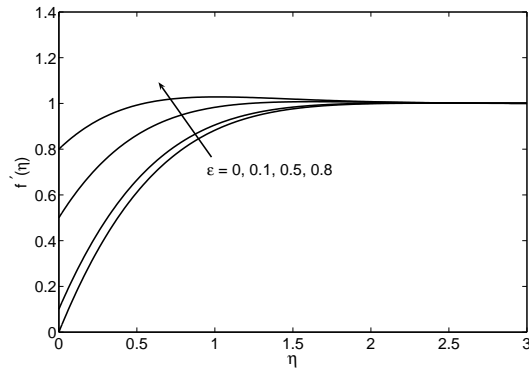


FIG. 8. Velocity profiles $f'(\eta)$ for different values of ε when $\lambda = 1$ (for the upper branch solution).

$\lambda = 1$ (assisting flow) are presented in Figs. 6 and 7. As seen in Figs. 4–7, the boundary conditions (2.11) are satisfied, which support the results presented in Tables 1 and 2 as well as Figs. 2 and 3, besides supporting the dual nature of the solutions to the boundary-value problem (2.9)–(2.11). The velocity profiles for different values of ε for the upper branch solution when $\lambda = 1$ are presented in Fig. 8. This figure shows that the velocity increases with the velocity ratio parameter ε ($= U_w/U_\infty$), and the velocity gradient at the surface is larger for smaller values of ε , which is consistent with the results presented in Fig. 1.

5. Conclusions

The problem of mixed convection flow near a two-dimensional stagnation-point on a vertical, continuously stretching sheet immersed in an incompressible viscous fluid has been investigated. Similarity solutions were obtained for the Navier–Stokes and energy equations, and the effects of the buoyancy and velocity ratio parameters on the flow field and heat transfer characteristics, for the case of Prandtl number unity, have been discussed. Results were presented for both the assisting and opposing flow regions. A new feature to emerge from the present investigation is the existence of dual solutions for the assisting flow, besides for the opposing flow that is usually reported in the literature. We also found that the flow separation from the surface was delayed if the sheet is stretched. It was also shown that solutions do not exist for the opposing flow if the magnitude of the buoyancy parameter is larger than the specific critical value.

Acknowledgements

The authors wish to express their very sincere thanks to the reviewers for the valuable comments and suggestions. This work is supported by a research

grant (SAGA project code: STGL-013-2006) from the Academy of Sciences Malaysia and a fundamental research grant (UKM-ST-01-FRGS0058-2006) from the Malaysia Higher Education Ministry.

References

1. K. HIEMENZ, *Der Grenzschicht an einem in den gleichförmigen Flüssigkeitsstrom eingetauchten geraden Kreiszyylinder*, Dingl. Polytech. Journal, **32**, 321–410, 1911.
2. N. RAMACHANDRAN, T.S. CHEN and B.F. ARMALY, *Mixed convection in stagnation flows adjacent to vertical surfaces*, ASME J. Heat Transfer, **110**, 373–377, 1988.
3. C.D.S. DEVI, H.S. TAKHAR and G. NATH, *Unsteady mixed convection flow in stagnation region adjacent to a vertical surface*, Heat Mass Transfer, **26**, 71–79, 1991.
4. Y.Y. LOK, N. AMIN, D. CAMPEAN and I. POP, *Steady mixed convection flow of a micropolar fluid near the stagnation point on a vertical surface*, Int. J. Numerical Methods Heat Fluid Flow, **15**, 654–670, 2005.
5. H.S. TAKHAR, A.J. CHAMKHA and G. NATH, *Unsteady mixed convection on the stagnation-point flow adjacent to a vertical plate with a magnetic field*, Heat Mass Transfer, **41**, 387–398, 2005.
6. T.C. CHIAM, *Stagnation-point flow towards a stretching plate*, J. Phys. Soc. Jpn., **63**, 2443–2444, 1994.
7. T.C. CHIAM, *Heat transfer with variable conductivity in a stagnation-point flow towards a stretching sheet*, Int. Comm. Heat Mass Transfer, **23**, 239–248, 1996.
8. T.R. MAHAPATRA and A.S. GUPTA, *Magnetohydrodynamic stagnation-point flow towards a stretching sheet*, Acta Mech., **152**, 191–196, 2001.
9. T.R. MAHAPATRA and A.S. GUPTA, *Heat transfer in stagnation-point flow towards a stretching sheet*, Heat Mass Transfer, **38**, 517–521, 2002.
10. R. NAZAR, N. AMIN, D. FILIP and I. POP, *Stagnation point flow of a micropolar fluid towards a stretching sheet*, Int. J. Non-Linear Mech., **39**, 1227–1235, 2004.
11. R. NAZAR, N. AMIN, D. FILIP and I. POP, *Unsteady boundary layer flow in the region of the stagnation point on a stretching sheet*, Int. J. Engng. Sci., **42**, 1241–1253, 2004.
12. C.H. CHEN, *Laminar mixed convection adjacent to vertical, continuously stretching sheets*, Heat Mass Transfer, **33**, 471–476, 1998.
13. T.Y. NA, *Computational Methods in Engineering Boundary Value Problems*, Academic Press, New York, 1979.
14. T. CEBECI and P. BRADSHAW, *Physical and Computational Aspects of Convective Heat Transfer*, Springer, New York, 1988.
15. T. CEBECI and P. BRADSHAW, *Momentum Transfer in Boundary Layers*. Hemisphere, Washington, 1977.
16. T. CEBECI, K.C. CHANG and P. BRADSHAW, *Solution of a hyperbolic system of turbulence-model equations by the “BOX” scheme*, Comp. Method Appl. Mech. Engng., **22**, 213–227, 1980.

17. A. ISHAK, R. NAZAR and I. POP, *Flow of a micropolar fluid on a continuous moving surface*, Arch. Mech., **58**, 529–541, 2006.
18. A. ISHAK, R. NAZAR and I. POP, *Dual solutions in mixed convection flow near a stagnation point on a vertical porous plate*, Int. J. Thermal Sciences, **47**, 417–422, 2008.
19. A. ISHAK, R. NAZAR and I. POP, *Dual solutions in mixed convection flow near a stagnation point on a vertical surface in a porous medium*, Int. J. Heat Mass Transfer, **51**, 1150–1155, 2008.
20. W. SCHNEIDER and M.G. WASEL, *Breakdown of the boundary-layer approximation for mixed convection above a horizontal plate*, Int. J. Heat Mass Transfer, **28**, 2307–2313, 1985.
21. W.R. SEARS and D.P. TELIONIS, *Boundary-layer separation in unsteady flow*, SIAM J. Appl. Math, **28**, 215–235, 1975.
22. N. AFZAL and T. HUSSAIN, *Mixed convection over a horizontal plate*, ASME J. Heat Transfer, **106**, 240–241, 1984.
23. F.R. HOOG, B. LAMINGER and R. WEISS, *A numerical study of similarity solutions for combined forced and free convection*, Acta Mechanica, **51**, 139–149, 1984.
24. A. RIDHA, *Aiding flows non-unique similarity solutions of mixed-convection boundary-layer equations*, J. Appl. Math. Phys. (ZAMP), **47**, 341–352, 1996.

Received September 3, 2007; revised version June 16, 2008.
